

# Extraction of Magnetite from Millscales Waste for Ultrafast Removal of Cadmium Ions

Nur Asyikin Ahmad Nazri, Raba'ah Syahidah Azis, Hasfalina Che Man, Ismayadi Ismail, Idza Riati Ibrahim

**Abstract:** This research was conducted to produce the magnetite ( $Fe_3O_4$ ) nanoparticles extracted from the industrial millscale waste. Then, the micron size samples were extracted and grounded on the high energy ball milling (HEBM) at various milling time for 4, 8, 12, 16 and 20 h. The formation of nanosized single-phase hexagonal spinel has been observed with XRD analysis as early as 4 h milling time. The FTIR transmission spectrum shows the appearance of a Fe-O functional group for each sample. HRTEM images showed that all the samples had a small particle size of 5-20 nm with uniform distribution. The specific surface area of the 5 adsorbents increased after the 8 h milling time and it showed reduction after that. The magnetite adsorbents then utilized the adsorbent in Cadmium ions removal of the aqueous solution.  $Fe_3O_4$  with 8 h milling time was able to remove 9.81 mg of cadmium ions with 1 g of adsorbents consume. The removal of the cadmium ions detected related to the particles size, surface areas and saturation magnetization. This research successfully revealed that the higher saturation magnetization contributed to high removal percentages in cadmium ions of aqueous solutions.  $Fe_3O_4$  extraction from mill scales waste is cost-effective, the process is eco-friendly and thus, potentially to be applied for wastewater treatment.

**Keywords:** Adsorption, cadmium, Magnetite, mill scales waste.

## I. INTRODUCTION

Magnetic separation is one of the promising methods as it is alternative method compared to the conventional method for the wastewater treatment [1]. Therefore, it is must be expected to lower the operation and production cost of the adsorbents, negligible risks of secondary contaminant and ultrafast adsorption time. According to this condition, magnetite ( $Fe_3O_4$ ) derived from mill scale waste would be the most potential magnetic adsorbent [2]-[5]. This magnetic adsorbent had been tested for the effectiveness in removal of ionic contaminant from an aqueous solution as reported

recently. The ionic contaminant can be either in the positive or negative contaminant.

The advantage of using magnetite is that it is amphoteric solid which is pH-dependent, where the surface charges varied due to the pH of the solution. Cadmium (Cd) is one of the non-essential nutrients recently present over the standard limit of water quality (0.03 mg/L) [6]. Thus, intense works on removing this contaminant were broadly studied by most of the wastewater researchers. Previously, researchers reported that the Cadmium ions were removed using different types of adsorbents such magnetic activated carbon that had efficiently remove the Cd ions [7]. However, the production of the adsorbents produced the second pollution when they use heat energy to burn and get the adsorbent. The secondary pollution occurs when the burning process releases a large amount of carbon dioxide ( $CO_2$ ). In addition, the time taken to remove the contaminant took a long time sometimes up to several weeks [2]-[4].

The magnetite had reported that it reached a plateau within 10 minutes of contact time. More recently, researchers found that processing the mill scales without the involvement of any chemicals might improve the performance of the adsorption even the adsorbent are in micron size. Unfortunately, it took 6 weeks to reach the equilibrium and to complete the adsorption [4]. This longer time of separation time would contribute to higher usage of electrical power to generate the external magnetic for the separation process. Upon this situation, the cost will increase and the mission to reduce the cost is still not achieved. Therefore, the great advantage goes to the adsorbent that can completely remove the heavy metals in a short time where the operational cost can be maintained. Summary of the reported adsorbents with the condition of good adsorbents is shown in Table I.

In current literature had reported that magnetic enriched particles can be extracted from millscale waste through the external magnetic field.

**Table I: Summary of reported adsorbents with the comparison of the production cost, secondary contaminant and adsorption time**

Adsorbent	Production Cost	Secondary contaminant	Adsorption time	Ref.
Magnetic AC	High	Yes	>1 h	[7]
Magnetic Particles (Millscale)	Low	No	>1 h	[2]-[4]
Magnetic Graphene	High	No	<1 h	[8]
Magnetic CNT	High	No	<1 h	[9]

Revised Manuscript Received on 20 October, 2019.

\* Correspondence Author

Nur Asyikin Ahmad Nazri, Center of Foundation Studies, Cawangan Selangor, Universiti Teknologi MARA & Institute of Advanced Technology (ITMA), Universiti Putra Malaysia, Selangor, Malaysia, asyikin2750@uitm.edu.my

Raba'ah Syahidah Azis, Physics Department, Faculty of Science, UPM & Institute of Advanced Technology (ITMA), Universiti Putra Malaysia, Selangor, Malaysia, rabaah@upm.edu.my

Hasfalina Che Man, Department of Biological and Agricultural Engineering, Faculty of Engineering, Universiti Putra Malaysia, Selangor, Malaysia, hasfalina@upm.edu.my

Ismayadi Ismail, Institute of Advanced Technology (ITMA), Universiti Putra Malaysia, Selangor, Malaysia, ismayadi@upm.edu.my,

Idza Riati Ibrahim, Institute of Advanced Technology (ITMA), Universiti Putra Malaysia, Selangor, Malaysia, idzariati@upm.edu.my

# Extraction of Magnetite from Millscales Waste for Ultrafast Removal of Cadmium Ions

This produced microparticles as the arsenate adsorbent [4].

In this study, magnetite was extracted from millscale waste by using high intensity of magnetic field and reduced size by using high energy ball mill (HEBM). HEBM is one of the simplest methods to reduce the size of the particles to the nanoparticles. The effect of the milling time was reported to affect the particles size, specific surface area, and the magnetic properties as well. All the five samples were then used in removing the Cd ions from the aqueous solution. The percentage of Cd ions removal showed a relation to the nature of each adsorbent. Therefore, magnetite extracted and purified from millscale waste had a great potential in the water purification system.

## II. METHODOLOGY

### A. Sample Preparation

#### Adsorbent

Raw waste industrial millscale were collected from steel factories located in Malaysia. Impurities such as stones, sands, dust or pieces of plastic are removed to avoid contamination in the samples. The mill scales were crushed using the conventional steel ball milling for 72 h. The milled powder was purified by using separation I: Magnetic Separation Technique (MST) for the magnetic and non-magnetic powder separation. Then, the magnetic powder was preceded with separation II: Curie Temperature Separation Technique (CTST) to extract magnetic compound  $\text{Fe}_3\text{O}_4$ . The waste mill scales separation routes (separation I and II) were carried out similar to the previous reports by Azis *et al.* [10] and with some modification. The magnetite ( $\text{Fe}_3\text{O}_4$ ) yielded to CTST is dried in the oven at  $60^\circ\text{C}$  for 24 h. The  $\text{Fe}_3\text{O}_4$  powder was milled at 1700 rotation per minutes (rpm) using SPEX 8000D milling machine with the ball to powder (BPR) ratio of 10:1 for 4, 8, 12, 16 and it takes 20 h to produce the nanometer size particles.

#### Adsorbate

All compound that was used to prepare the reagent solutions is known as an analytical reagent grade. The stock solution to Cadmium nitrate ( $\text{Cd}(\text{NO}_3)_2$ ) (Sigma-Aldrich, UK) (5.0 mg/L) is prepared by dissolving a weighed quantity of the respective  $\text{Cd}(\text{NO}_3)_2$  in deionized water. The concentration of the metal solution and pH used for the experiment is 1.0 mg/L with pH 7 respectively.

### B. Adsorbents Characterization

The structural and phase composition of samples were analyzed with X-ray diffraction (Philips Expert PW3040 diffractometer) operating in 40 kV and 40 mA with  $\text{CuK}\alpha$  radiation ( $\lambda = 0.154 \text{ nm}$ ). The morphology, particles size and atom arrangement of the samples were observed using a JEM JEOL 2100 HR transmission electron microscope. Brunner Emmet Teller (BET): Micromeritics Tristar II PLUS BET machine used to determine the surface area per mass of samples. Samples were degassed at  $120^\circ\text{C}$  around 0.2 mg for 8 hours of 1 Pa vacuum condition before the measurement to remove samples humidity.

Fourier transform infrared (FTIR) spectrometer (Thermo Nicolet, Model Nicolet 6700) spectroscopic analysis ( $200\text{-}4000 \text{ cm}^{-1}$ ) were recorded to detect the functional group in the powder. The magnetic properties of samples were measured using a VSM (LAKESHORE Model 7404). The measurement was carried out at room temperature by applying an external field of 0 - 13 kG parallel to the sample. Full operation is shown in Fig.1.

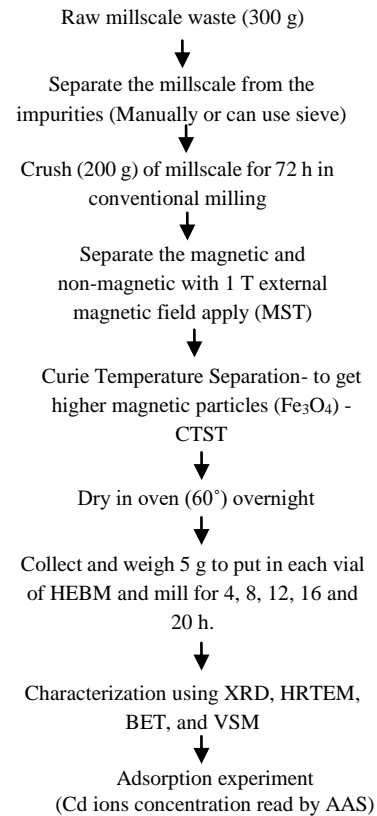


Fig.1: Operational scheme of this work

### C. Adsorption Experiment

30 mg of  $\text{Fe}_3\text{O}_4$  nanoparticles adsorbent was added to the 100 ml of Cd solution and placed in the vibrator bath (Variable speed reciprocal vibrator, model HY-8) with fixed 160 rpm for 20 min. All the adsorptions tests were carried out at room temperature around  $22\text{-}25^\circ\text{C}$  in a shaker by mixing accurate adsorbents weight amounts with adsorbate solutions to specific concentrations of a covered bottle. The pH value of the solution was maintained at pH 7.

The Cd ions concentration adsorption capacities of solutions were determined using the atomic absorption spectrometer (AAS) (Thermo Scientific iCE 3000 Series Solaar AA) The adsorbate amounts were taken up by an adsorbent as the concentration function of adsorbate at a constant temperature. It is called the adsorption capacity and calculated as (1). Percentage of Cd ions removal is calculated as (2):

$$q_e = \frac{V}{m} (C_o - C_e)$$

(1)



$$\%Cd\ Removal = \frac{C_o - C_e}{C_o} \quad (2)$$

where  $q_e$  (mg/g) is the amount of adsorbate per unit mass of adsorbent at time  $t$ .  $C_o$  and  $C_e$  are the initial and equilibrium concentrations (mg/L) of the solution respectively.  $V$  is the solution volume in liters and  $m$  is the adsorbent mass in grams (g). In this experiment, the initial concentration used was 1.0 mg/L. The pH of the solution was measured using the pH meter.

### III. RESULT AND DISCUSSION

#### A. Structural and Microstructural Analysis

Fig.2 shows the XRD spectra subjected to samples after HEBM for 4, 8, 12, 16 and 20 h, respectively. As revealed, diffraction peaks of all samples after HEBM completely corresponded to the standard pattern characteristic peaks of the magnetite hexagonal inverse spinel structure (JCPDS: 98-005-9302) at  $30.1^\circ$  (110),  $35.45^\circ$  (113),  $43.07^\circ$  (024),  $56.97^\circ$  (125),  $62.47^\circ$  (208). XRD peaks for all samples are consistent which suggests that HEBM process is effective in protecting the  $Fe_3O_4$  nanoparticles from oxidation. This result was entirely consistent with the published data [11].

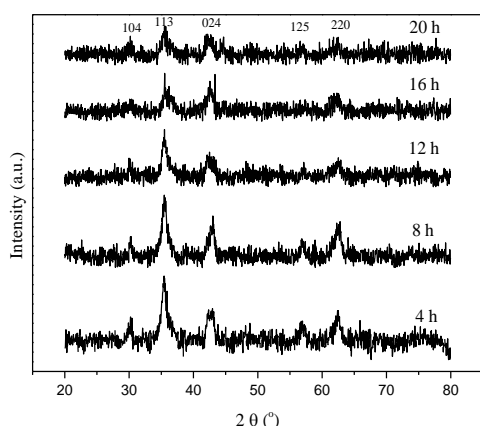


Fig. 2: XRD patterns of samples after HEBM for 4, 8, 12, 16 and 20 h

As seen from the spectra, the main peak that corresponded to  $hkl$  (113) is broadened when the milling time is prolonged. The broadened diffraction peaks might be contributed by the instrumental radians and might be due to the smaller particle size and lattice strain [11]. The collision occurred between balls, walls and an impacted powder particle during high energy ball milling that induced stress of the powder particles [12]. This results in lowering the crystallites of the samples and reducing the particle sizes. Equation (3) relates to the broadening of the diffraction peaks and the particle size [13]:

$$B = \frac{k\lambda}{t} \cos\theta \quad (3)$$

Where  $B$  is the broaden width,  $k$  is a constant,  $\lambda$  is the x-ray wavelength,  $t$  is the particle size and  $\theta$  is the diffraction angle.

Fig. 3 shows HRTEM images of  $Fe_3O_4$  after 8 h milling with different magnifications, which demonstrated an aggregation occurred between the  $Fe_3O_4$  nanoparticles ranging of 5 – 20 nm in size. The particle sizes are encountered to lessen as the milling time increased after the HEBM process of 4 to 20 h as can be seen in Table II.

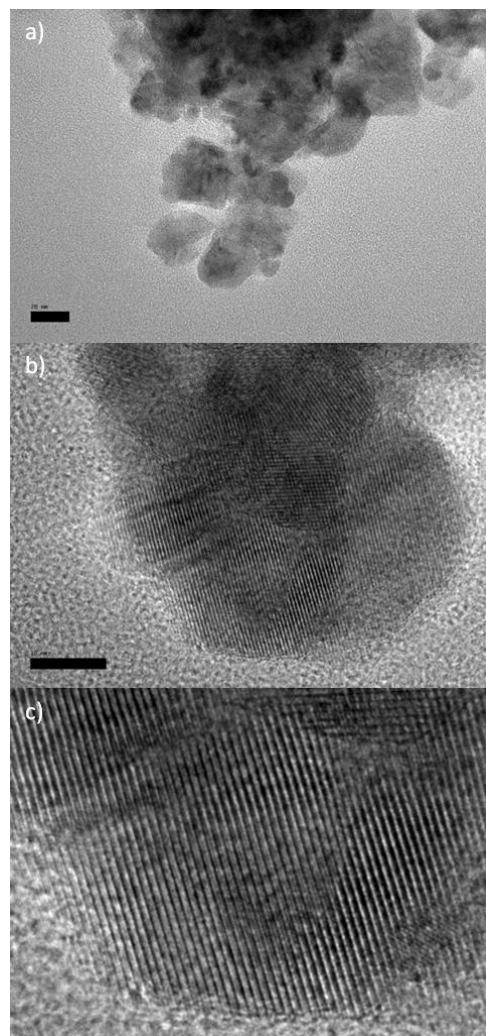


Fig. 3: HRTEM images for samples after 8 hours milling time (a) 20 nm scale bar, (b) 10 nm scale bar and (c) zoom in the lattice of the  $Fe_3O_4$

Table II: The XRD parameters of crystallite size and HRTEM particle size

Adsorbent	Crystallite size, $d_{XRD}$ (nm)	HRTEM particle size, $d_{TEM}$ (nm)
4 h	16.7	16.2
8 h	13.3	13.1
12 h	11.2	10.9
16 h	6.7	6.3
20 h	6.5	6.5

The agglomeration of the nanoparticles indicating good connectivity between the grains due to the large surface area, higher magnetic forces and subjected to cold welding and fracturing of the HEBM process.

The agglomeration was reduced with an increase in particle size

[14]. The lattice distributed substantially over some dislocation occurs subjected to the HEBM.

All particles size is compared with the crystallite size as shown in Table II. The particle size obviously reduced from microparticles to nanoparticles size after the HEBM. No significant difference can be measured when prolonged the milling time, which only resulted in a small difference between each particle size (<5 nm). However, HEBM for 20 h showed the size started to slightly increase. The crystallite size was calculated using Scherrer's equation in the X'Pert HighScore Plus Software. It is empirically found that the average particle size depends on the milling time as in (4).

$$D = 2.97 \exp \frac{25}{t + 6.27} \quad (4)$$

Where  $D$  is the average particle size (nm),  $t$  is the milling time (h). Therefore, prolonged the milling time which would expect to lower the size of the particles. However, [14] reported that it will reach a maximum point and after that, the size had the possibility to expand.

### B. FTIR Analysis

Fig. 4 shows the FTIR transmittance spectra of the samples. The spectra for 4, 8, 12, 16 and 20 h samples presents a band at  $532 \text{ cm}^{-1}$  (in the  $\text{Fe}_3\text{O}_4$  transmission region) [15], [16]. The FTIR shows the vibration characteristic dominated by the Fe-O [17]. These results in a close agreement with theoretical values and indicate the sample  $\text{Fe}_3\text{O}_4$  nanoparticles. The transmittance band at  $532 \text{ cm}^{-1}$  is associated with the stretch and torsional vibration mode of Fe-O bonds in the tetrahedral and octahedral sites. Compared to the literature, the two IR peaks of the samples are shifted to higher wavenumbers due to the ultrafine particle sizes [17]. Peak 2360 and  $3700 \text{ cm}^{-1}$  showed that the ability of the magnetite to absorb water molecules [18].

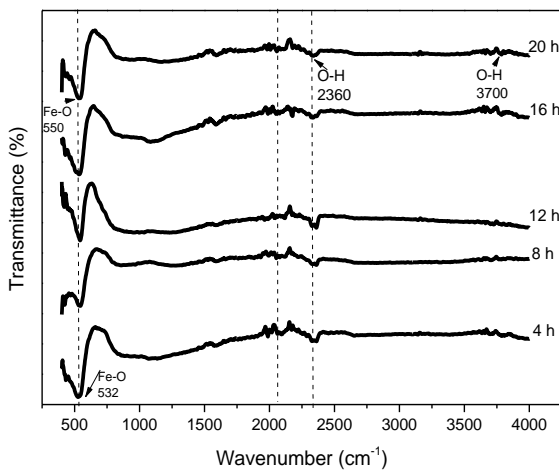


Fig. 4: FTIR transmittance pattern for milled  $\text{Fe}_3\text{O}_4$  at 4, 8, 12, 16 and 20 h

In the event the magnetite ( $\text{Fe}_3\text{O}_4$ ) size particles reduced to nanoscales dimensions, the bond force increased constantly due to large numbers involved in the surface atoms being broken that resulted in the rearrangement of non-localized electrons on the particle surface [15].

Therefore, the FTIR spectrum of  $\text{Fe}_3\text{O}_4$  nanoparticles exhibits a blue shift whereby the characteristic absorption bands of the Fe-O bond shifted to a higher wavenumber by around  $550 \text{ cm}^{-1}$ .

### C. Magnetic Analysis

The parameters such as saturation magnetization  $M_s$  and coercivity  $H_c$  were determined from the magnetization curves ( $M-H$ ). The result is presented in Fig. 5. The particles are a single domain in which thermal energy was unable to overcome the anisotropy energy barrier for reversals spins and exhibiting the typical ferrimagnetic behavior [14],[15]. However, the hysteresis showed the behavior falls into ferrimagnetism range that resulted in significant values of coercivity,  $H_c$ .

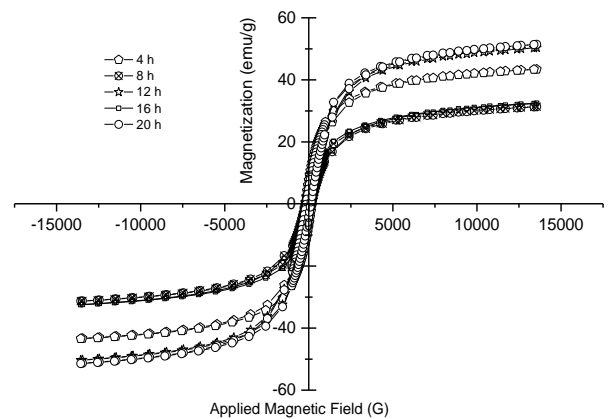


Fig. 5: Magnetic hysteresis loops for each sample

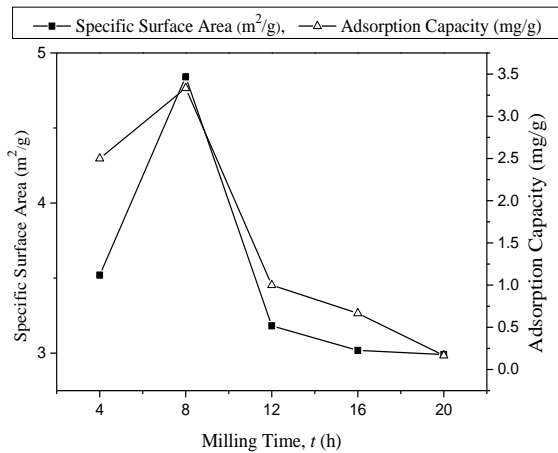
Therefore, the mixture behavior of superparamagnetism and ferrimagnetism were simultaneously observed in the samples. The mixture expected to occur as to the particle size distribution (see Fig. 3) where there are some particles of multidomain range ( $>20 \text{ nm}$ ) [11]. In this case, all the samples show a mix of ferrimagnetism and superparamagnetism behavior with good standing of the saturation magnetization values. Besides, the shape also affects the behavior of the magnetic particles.

### D. Specific surface area and porosity

The specific surface area was determined using isothermal nitrogen adsorption method. Fig. 6 shows that at early 4 h and 8 h milling time, the  $\text{Fe}_3\text{O}_4$  had a larger surface area due to the mechanical activation. However, after reaching a specific surface area at 8 h samples, the surface area decreased and almost became static to a point. This result is in agreement with the report previously [15].

$\text{N}_2$  adsorption-desorption isotherms of  $\text{Fe}_3\text{O}_4$  are shown in Fig. 7. According to the graph, the  $\text{N}_2$  adsorption-desorption curve of  $\text{Fe}_3\text{O}_4$  nanoparticles displayed type III with hysteresis corresponding to the capillary condensation which is typical for micropores material [14]. Type III explained the adsorption is on physisorption without chemical changes which occurred between the

adsorbent and adsorbate. Physisorption may be either the Van de Waals forces or Coulombic forces specificity at low degree [15].



ig. 6: Graph of the specific surface area and adsorption capacity,  $q_e$  as a various milling time function

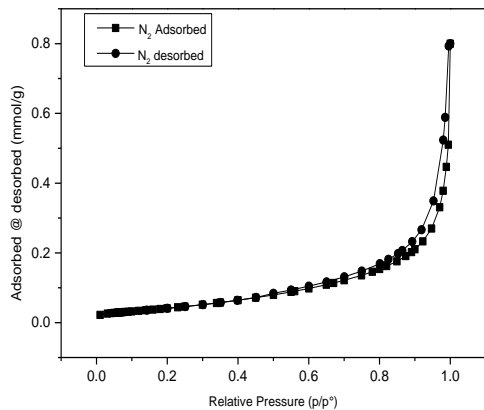


Fig. 7: N<sub>2</sub> adsorption-desorption isotherm of Fe<sub>3</sub>O<sub>4</sub>

### E. Adsorption Analysis

Fig. 8 demonstrates that the adsorption reaches a plateau after 10 mins of contact time. It can be seen clearly that Fe<sub>3</sub>O<sub>4</sub> milled 8 h gave the highest Cd ions removal percentage followed by 4, 12, 16 and 20 h. Based on Fig. 9, it clearly showed the adsorption capacity is in relation to the magnetization of the Fe<sub>3</sub>O<sub>4</sub> nanoparticles.

In addition, the saturation magnetization also may contribute to higher removal of Cd ions. The graph demonstrated that the saturation magnetization  $M_s$  influenced the rapid and higher value of adsorption. The adsorption capacity, size and surface area are left to drop throughout the prolonging milling time. Therefore, 8 h milling hour sample showed the best performance in removing Cd ions with 97 % Cd ions removal and 3.33 mg/g adsorption capacity. Magnetite is reported as an amphoteric solid that can be easily protonated or deprotonated. This will result in the pH-dependent surface charge. Whereby if it develops charges in protonation ( $\text{Fe-OH} + \text{H}^+ \leftrightarrow \text{Fe-OH}_2^+$ ) it will become positively charged, while when deprotonation ( $\text{Fe-OH} \leftrightarrow \text{Fe-O}^- + \text{H}^+$ ) occurs, it will be negatively charge [13].

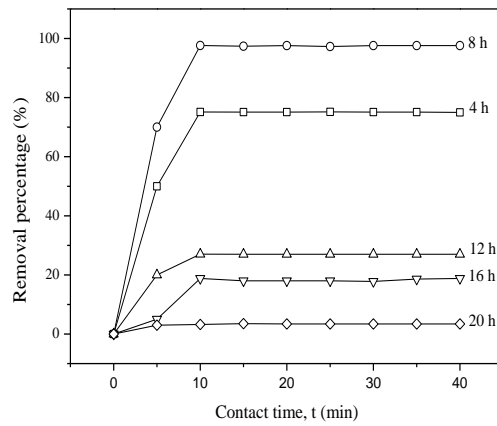
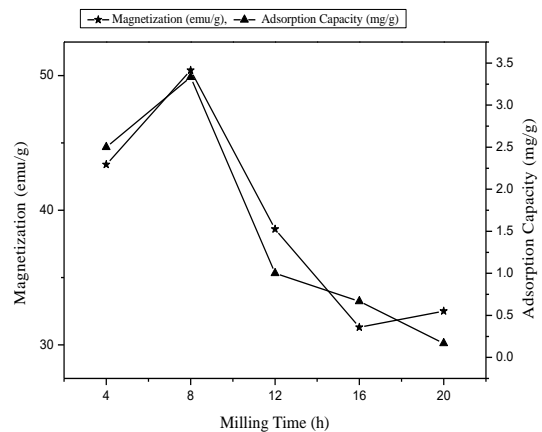


Fig. 8: Effect of contact time to the Cadmium removal with initial concentration 1 mg/L, adsorbent dosage 0.3 mg/L at pH 7

F



Fi

g. 9: Magnetization and adsorption capacity as a function of various milling time

The 8 h milling hour is the optimum milling time to produce the best adsorption capacity. Prolonging the milling time will lower the removal of Cd ions which in relation to the  $M_s$  and the specific surface area. This might be related to the significant surface areas as shown previously (see Fig. 6).

### IV. CONCLUSION

This study proved the millscale waste has good potential to be used in Cd ions removal in the aqueous solution. Research successfully turned the waste mill scales into a mass volume of magnetite nanoparticles with high magnetic attraction characteristics. HEBM technique supports to refine the particles size as good distribution of Fe<sub>3</sub>O<sub>4</sub> nanoparticles and also at reducing the size. The adsorption capacity of the best milling time producing magnetite is at 8 h which are 3.33 mg/g. Further research should be continued with respect to the utilization of mill scales waste of Cd ions removal of the wastewater treatment plant such as regeneration and reuse of the sorption-desorption cycles.



## ACKNOWLEDGEMENT

This work was supported by Universiti Putra Malaysia Grants (Putra Initiative Grants (UPM/700-1/2/GPPI/2017/9541600), Impact Putra Gants (GP-IPS/2017/9580600) and the Ministry of Education Malaysia (Fundamental Research Grants Scheme (FRGS) (No. 5524942). Thanks to the Department of Physics, Faculty of Science, MSCL ITMA and Centre of Foundation Studies (Selangor branch), UiTM and the Department of Biological and Agricultural Engineering, Faculty of Engineering, UPM for the measurements facilities.

## References

1. N.A.A.Nazri, RS. Azis, AH Saari, I.Ismail and H.Cheman, "Role of Magnetite Nanoparticles for Metal Absorbents in Waste Water Treatment" in Emerging Themes Fundamental and applied science, UPM Press, pp. 47-52, 2018.
2. M. K. Shahid, S. Phearom, and Y. G. Choi, "Synthesis of magnetite from raw mill scale and its application for arsenate adsorption from contaminated water," *Chemosphere*, vol. 203, pp. 90–95, 2018.
3. H. Chun, and Y. Choi, "A Study on the Mill Scale Pretreatment and Magnetite Production for Phosphate Adsorption," *Journal of Korean Society of Environmental Engineers*, vol. 37, pp. 246-252, 2015.
4. M. K. Shahid, S. Phearom, and Y. G. Choi., "Adsorption of arsenic (V) on magnetite-enriched particles separated from the mill scale," *Environmental earth sciences*, vol. 78, pp. 65 , 2019.
5. J. E. Doliente, Y. Kim, H. Nam, and Y. Choi, "Mill Scale-Derived Magnetite Particles: Effective Adsorbent for the Removal of Phosphate in Aqueous Solutions," *Journal of Environmental Engineering*, vol. 143, no.12, pp. 04017076, 2017.
6. O. Faroon, A. Ashizawa, S. Wright, P. Tucker, K. Jenkins, L. Ingerman, and C. Rudisill, "Toxicological profile for cadmium," *Agency for Toxic Substances and Disease Registry*, pp.1-487, 2012.
7. Gu, S. Y., Hsieh, C. T., Gandomi, Y. A., Yang, Z. F., Li, L., Fu, C. C., & Juang, R. S., "Functionalization of activated carbons with magnetic Iron oxide nanoparticles for removal of copper ions from aqueous solution," *Journal of Molecular Liquids*, vol. 277, pp. 499-505, 2019.
8. A. I. A. Sherlala, Raman, A. A. A. Raman, M. M. Bello, and A. Asghar, "A review of the applications of organo-functionalized magnetic graphene oxide nanocomposites for heavy metal adsorption," *Chemosphere*, vol. 193, pp. 1004-1017, 2018.
9. B. Ranjan, S. Pillai, K. Permaul, and S. Singh, "Simultaneous removal of heavy metals and cyanate in a wastewater sample using immobilized cyanate hydratase on magnetic-multiwall carbon nanotubes," *Journal of Hazardous Materials*, vol. 363, pp. 73-80, 2019.
10. R. S. Azis, M. Hashim, N. Yahya, N. M. Saiden, "A Study of Sintering Temperatures Variation on Microstructure Developments of Strontium Hexaferrite Millscale-Derived," *Journal of Applied Sciences*, vol. 2, no. 12, pp. 1092-1095, 2002.
11. U. Schwertmann, and R. M. Cornell, *Iron oxides in the laboratory: preparation and characterization*, John Wiley & Sons, 2008.
12. E. Purushotham, and N. G. Krishna, "Effect of particle size and lattice strain on Debye-Waller factors of Fe 3 C nanoparticles," *Bulletin of Materials Science*, vol. 37, no. 4, pp. 773-778, 2014.
13. G. S. Parkinson, "Iron oxide surfaces," *Surface Science Reports*, vol. 71, no. 1, pp. 272-365, 2016.
14. A. H. Emami, M. S. Bafghi, J. V. Khaki, and A. Zakeri, "The effect of grinding time on the specific surface area during intensive grinding of mineral powders," *Iranian Journal of Materials Science and Engineering*, vol. 6, no. 2, pp. 30-36, 2009.
15. T. T. Bui, X. Q. Le, D. P. To, and V. T. Nguyen, "Investigation of typical properties of nanocrystalline iron powders prepared by ball milling techniques," *Advances in Natural Sciences: Nanoscience and Nanotechnology*, vol. 4, no.4, pp. 045003, 2013.
16. E. Poinern, S. Brundavanam, S. K. TripathySuar, and D. Fawcett, "Kinetic and adsorption behaviour of aqueous cadmium using a 30 nm hydroxyapatite based powder synthesized via a combined ultrasound and microwave based technique," *Physical Chemistry*, vol. 6, pp.11-22, 2016.
17. A. H. Ali, "Comparative study on removal of cadmium (II) from simulated wastewater by adsorption onto GAC, DB, and PR," *Desalination and Water Treatment*, vol. 51, pp. 5547-5558, 2013.
18. P. L. King, M. S. Ramsey, P. McMillan, and G. A. Swayze, "Laboratory Fourier transform infrared spectroscopy methods for geologic

samples," in *Infrared Spectroscopy in Geochemistry, Exploration, and Remote Sensing*, CA: Mineralogical Association of Canada, pp. 57-91, 2004.

## AUTHORS PROFILE



**Nur Asyikin Ahmad Nazri**, is a Ph.D. student of Materials Synthesis and Characterization Laboratory (MSCL) at the Institute of Advanced Technology (ITMA), Universiti Putra Malaysia (UPM). Her skills and interest are nanomaterials and magnetic materials. She is a Lecturer at Center of Foundation Studies, UiTM Selangor, Malaysia. She had published in a chapter in Book, and Conference. Her current research is on magnetic nanoparticle as adsorbents for wastewater treatment.



**Raba'ah Syahidah Azis (Ph.D.)** is an Associate Professor at the Department of Physics, Universiti Putra Malaysia. She is an Associate Researcher at the Material Synthesis and Characterization Laboratory (MSCL), Institute of Advanced Materials (ITMA), UPM. She is also an Auditor of Malaysian Solid State Science and Technology (MASS). Her research interest in material synthesis and characterization specialized in magnetic materials, nanomaterial, ferrites, magnetic materials used in the wastewater treatment process (WWTP) and radar adsorbing materials (RAM).



**Ismayadi Ismail (Ph.D.)**, is a Research Officer at the Institute of Advanced Materials (ITMA), Universiti Putra Malaysia, Selangor, Malaysia. He is an active member of Malaysian Solid State Science and Technology (MASS). His research skills and expertise are nanomaterial and microstructure.



**Hasfalina Che Man (Ph.D.)** is an Associate Professor at the Department of Biological and Agricultural Engineering, Faculty of Engineering, UPM. She is also a Chartered Engineer of IChemE ((Institution of Chemical Engineers). Her research interests are bio-environmental engineering, environmental engineering, wastewater treatment, and agriculture waste management.



**Idza Riati Ibrahim** is a Post-doctoral Researcher at Institute of Advanced Technology (ITMA), Universiti Putra Malaysia. She received her BSc (Hons) and MSc in Materials Science in 2007 and 2012 respectively from Universiti Putra Malaysia (UPM). She then gained her PhD in Nanomaterials and Nanotechnology from the same university in 2017. Idza Riati Ibrahim has served more than 5 years as a temporary demonstrator and tutor at Department of Physics, Faculty of Science, UPM and Centre of Foundation Studies for Agricultural Science in subject Physics 1, Physics 2, Metals and Alloys, Ceramics and Polymers, Introduction to Mechanics, Thermal Physics, Waves and Optics. In addition, she also has extensive experience in research as she has previously served as an research enumerator and now is serve as a post-doctoral researcher. Her research interests are on Magnetic Materials, Microwave Absorbing Materials, Nanomaterials and Nanotechnology. She has also published her works in high impact journals and has presented her research at local, regional and international seminars. Recently, she has been awarded with 2 golds and 2 silver medals in Materials Technology Challenge after presented her works on microwave absorbing materials.

